

----- Supporting Information -----

# Xylene Selectivity at the External Surface of Hierarchical Zeolites: Experiment and Molecular Modeling

*Izabel C. Medeiros-Costa<sup>†</sup>, Catherine Laroche<sup>†</sup>, Benoit Coasne<sup>‡</sup>, Javier Pérez-Pellitero<sup>†\*</sup>*

<sup>†</sup> IFP Energies nouvelles, Rond-point de l'échangeur, BP3, 69360 Solaize, France

<sup>‡</sup> Univ. Grenoble Alpes, CNRS, LIPhy, F-38000 Grenoble, France

# S1. General complimentary data

**Table S1.** Unit cell composition of different samples. Ba content and Si/Al ratio were determined by X-ray fluorescence. The last line corresponds to the composition of the unit cell of the model used in the simulations.

Sample	Unit cell composition
NA-1	$Ba_{37.4}Na_{17.0}O_{384.0}Al_{91.9}Si_{100.1}$
NA-2	$Ba_{36.1}Na_{20.1}O_{384.0}Al_{92.3}Si_{99.7}$
NA-3	$Ba_{38.4}Na_{13.3}O_{384.0}Al_{90.1}Si_{101.9}$
LL	$Ba_{37.7}Na_{16.1}O_{384.0}Al_{91.4}Si_{100.6}$
Conventional X	$Ba_{37.1}Na_{15.6}O_{384.0}Al_{89.7}Si_{102.3}$
Model/simulation	$Ba_{48.0}O_{384.0}Al_{96.0}Si_{96.0}$

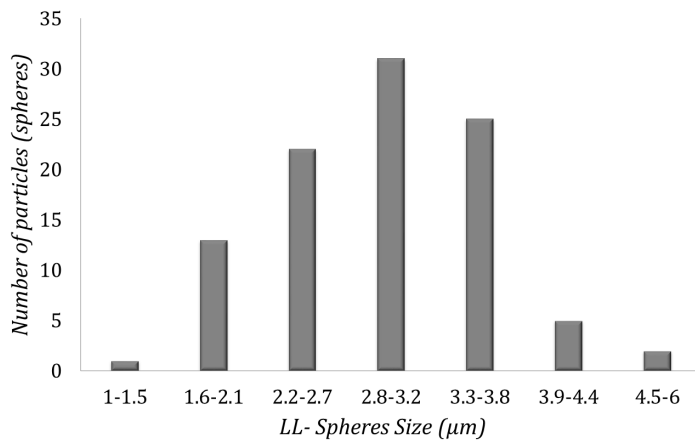
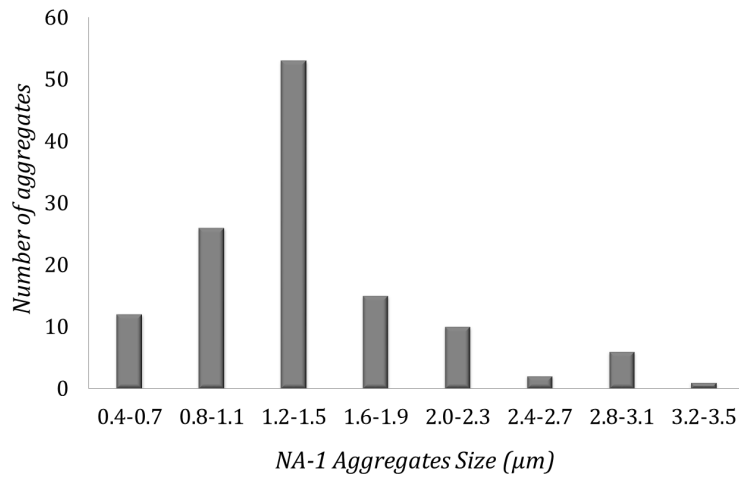


**Figure S1.** Size distribution of NA-1 aggregates (top) and LL spheres-like particles (bottom).

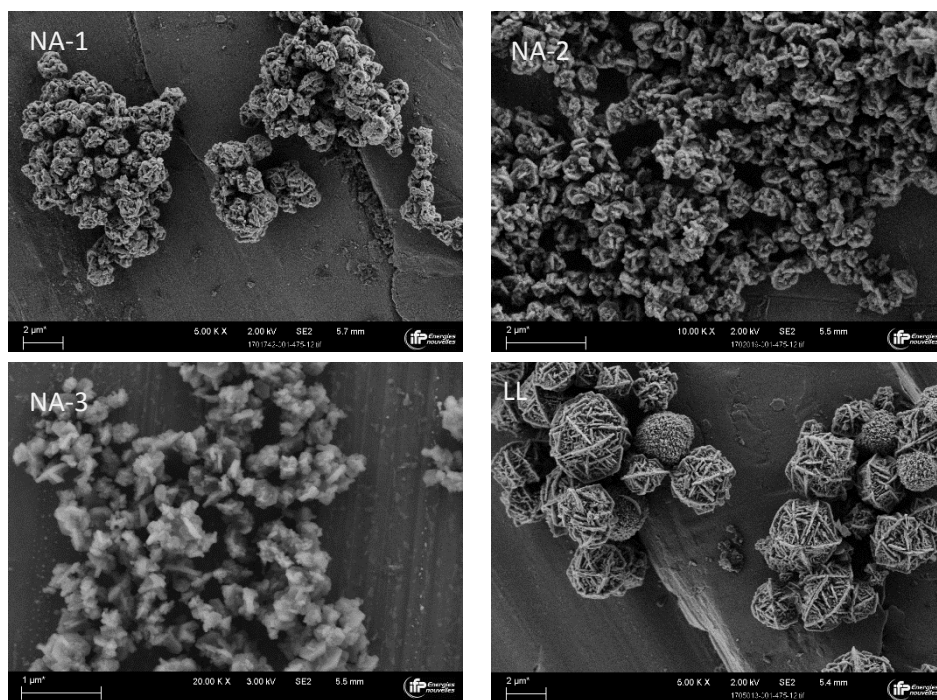


**Figure S2.** Scanning electron micrographs of samples NA-1, NA-2, NA-3 and LL. From these images, it can be seen that the size of the aggregates in NA-2 and NA-3 is smaller than those of NA-1. The spheres-like particles in LL sample present largest size among the other zeolites.

## S2. Complementary Adsorption Data

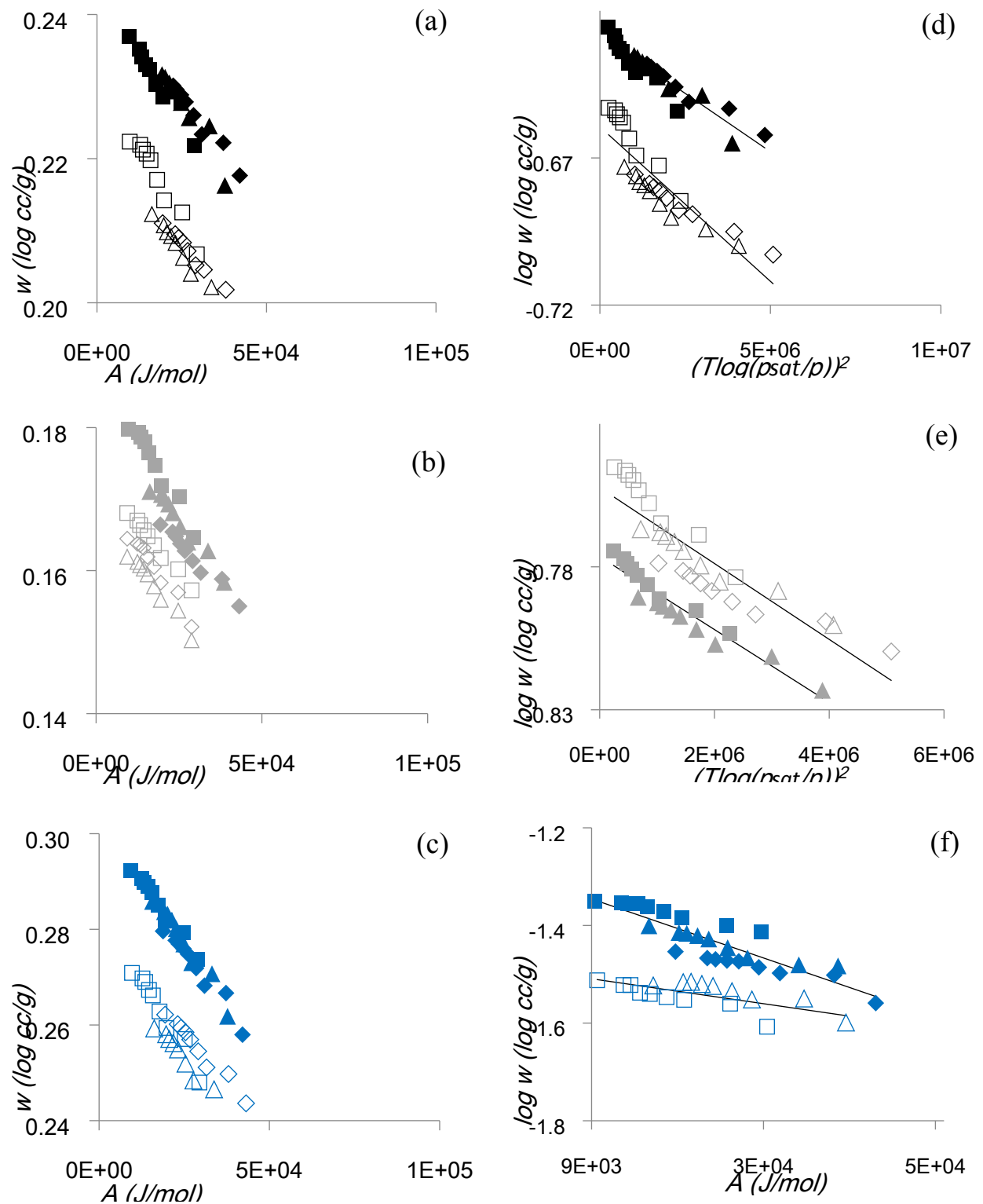


**Figure S3.** Characteristic adsorption curves for  $px$  and  $ox$  in conventional and hierarchical zeolites: (a) conventional, (b) LL and (c) NA-3. Linear plot of Dubinin-Radushkevich equation for  $px$  and  $ox$  in the conventional and hierarchical zeolites: (d) conventional and (e) LL. Linear plot of the characteristic curve equation for nonporous materials for  $px$  and  $ox$  on the surface of hierarchical NA-3 zeolite (f). Filled and empty

symbols indicate the adsorption of *px* and *ox*, respectively. The different temperatures correspond to symbols: squares (100°C), triangles (150°C) and diamonds (175°C).

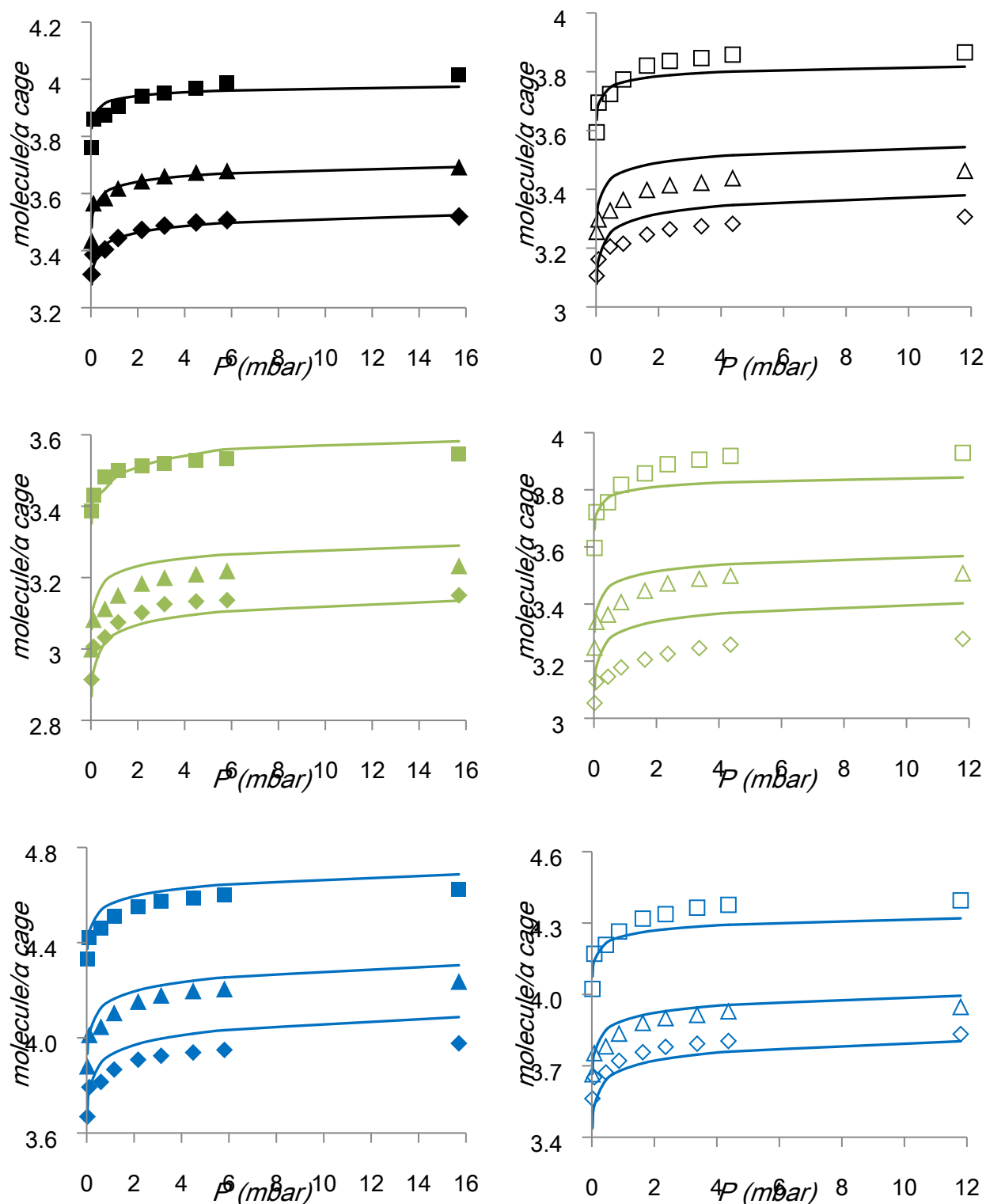


**Figure S4.** Comparison between experimental data and model for adsorption isotherms of *px* and *ox* on conventional and hierarchical BaX zeolites: conventional BaX zeolite (black), LL BaX zeolite (green) and NA-3 BaX zeolite (blue). Filled and empty symbols indicate the adsorption of *px* and *ox*, respectively. The different temperatures can be identified by symbols: squares (100°C), triangles (150°C) and lozenges (175°C).

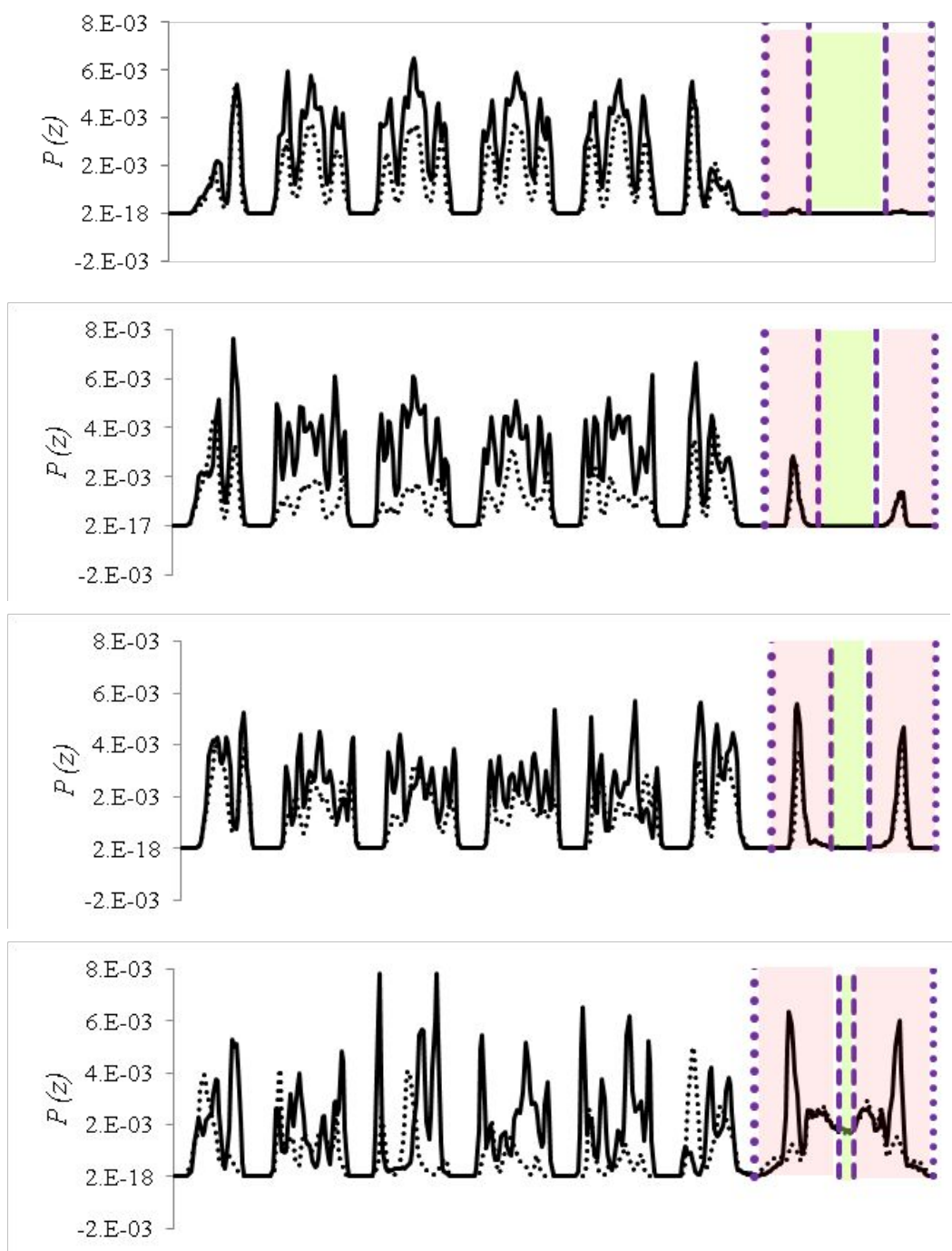


**Figure S5.** Probability density distribution profiles for  $px$  (solid line) and  $mx$  (dotted line) obtained for the adsorption at  $175^\circ\text{C}$  of an equimolar binary mixture in a Ba zeolite bearing an external surface. The different total pressures considered are (from top to bottom):  $P = 5 \times 10^{-4}$ ,  $2 \times 10^{-2}$ , 5 and 100 mbar. The corresponding loadings are respectively 1.3, 2.7, 3.3 and 3.9 molecules per  $\alpha$  cage. Pink and green zones represent the surface and bulk-fluid phases. The dotted and dashed purple lines indicate the zeolite crystal/surface and surface/bulk fluid interfaces, respectively.

## ***S3. GCMC simulations of xylene adsorption***

### ***S3.1. Methods***

GCMC (Grand Canonical Monte Carlo) simulations combined with a bias scheme for the insertion of the center of mass of the guest molecules were performed to calculate the adsorption isotherms with the GIBBS code v.9.3. Systems were allowed to equilibrate for at least ten million MC steps followed by production runs of at least 100 million MC steps. The atomic positions of the solid were frozen during the simulations. This allowed the construction of a guest-host interaction energy grid prior to the MC simulations. All simulations were performed in a simulation box incorporating at least the equivalent of 8 bulk unit cells. the general form of the force field is reduced to a simplified expression of the total energy  $U$  only based on the summation of two different contributions accounting for the dispersion-repulsion and the electrostatic interaction interactions:

$$U = U_{LJ} + U_{elec} \quad (\text{Eq SI 1})$$

Although it is well known that the origin of the  $px$  selectivity in some zeolitic forms arises from an entropic contribution, it is worth mentioning the importance of the electrostatic contribution when dealing with counter-cationic species and aromatic hydrocarbons. The first contribution, corresponding to the dispersion-repulsion energy, is described *via* a Lennard-Jones potential between two atomic sites  $i$  and  $j$ :

$$U_{LJ}^{ij}(r) = 4 \varepsilon_{ij} \left[ \left( \frac{\sigma_{ij}}{r_{ij}} \right)^{12} - \left( \frac{\sigma_{ij}}{r_{ij}} \right)^6 \right] \quad (\text{Eq SI 2})$$

where  $\varepsilon_{ij}$  is the potential energy depth,  $r_{ij}$  is the distance between two particles,  $\sigma_{ij}$  is the distance between two particles where the potential energy equals zero. The first term  $(\sigma_{ij}/r_{ij})^{12}$  describes repulsive interactions while the second term  $(\sigma_{ij}/r_{ij})^6$  correspond to attractive interactions

The second contribution, corresponding to electrostatic interactions, simply involves a coulombic term:

$$U_{elec}^{ij}(r) = \frac{q_i q_j}{4\pi\epsilon_0 r_{ij}^2} \quad (\text{Eq SI 3})$$

where  $\epsilon_0$  is the vacuum permittivity,  $q_i$  is the electric charge of a site  $i$  and  $r_{ij}$  is the distance between the two point charges.

LJ interactions and real space electrostatic contributions were calculated using a cutoff radius of 20 Å. No Lennard-Jones tail corrections were considered; however, standard long-range electrostatic interactions were calculated using the Ewald methodology with 9 vectors on the reciprocal space and a screening factor  $n = 2.5$ . The crystallographic positions of the different atoms for both materials were taken from the data available in the Materials Studio software.<sup>1</sup>

The isosteric heats of adsorption  $q_{st}$  were calculated according to:

$$q_{st} = H_b - \left[ \frac{\delta U_a}{\delta N} \right]_{T,V} \quad (\text{Eq SI 4})$$

where  $H_b$  is the enthalpy of the bulk phase,  $U_a$  is the energy of the adsorbed phase, and  $N$  the number of adsorbed molecules. Using a fluctuation method with ideal gas assumptions under Henry's regime, the isosteric heats can be readily calculated from GCMC simulation according to:

$$q_{st} = RT - \frac{\langle U_{ext}^s N \rangle - \langle U_{ext}^s \rangle \langle N \rangle}{\langle N^2 \rangle - \langle N \rangle^2} \quad (\text{Eq SI 5})$$

where  $U_{ext}^s$  is the intermolecular energy of the adsorbed phase. The brackets denote averages in the grand canonical ensemble.

### **S3.2. Xylene force field**

The adsorbate molecules are described according to the electrostatic version of the anisotropic united atom (AUA) for aromatics.<sup>2</sup> Inspired from the work of Peralta *et al.*<sup>3</sup> and to avoid charges collapse between the ring-centered quadrupole and the counter-cations, slight modifications were introduced to distribute the electrostatic interaction around the totality of the aromatic ring. A schematic representation of the implementation of the model is shown in Figure S. The different parameters used in the calculations are listed in Table SS2.

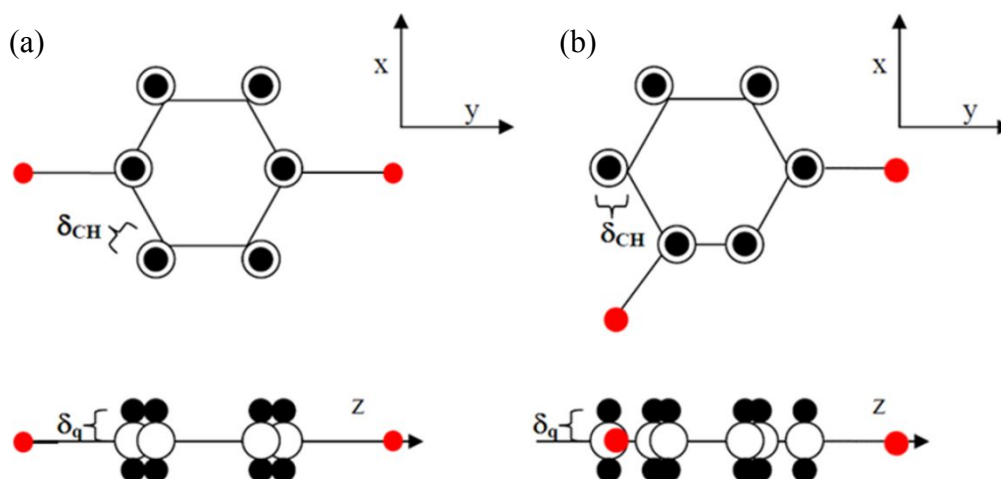


**Figure S6.** Schematic representation of the implementation of the electrostatic version of the AUA potential for  $px$  (a) and  $mx$  (b). Adapted from Ref. 3.

**Table S2** Lennard-Jones parameters and electrostatic point charges of the adsorbate molecules.

Force center	$\sigma^\dagger$ [Å]	$\varepsilon/k_b^\dagger$ [K]	$\delta^{\dagger\dagger}$ [Å]	$\delta_q^{\dagger\dagger\dagger}$ [Å]	q [e]
CH3-AUA	3.6072	120.15	0.21584	---	0.025
CH-arom-AUA_elec	3.361	75.6	0.315	0.4	1.355/-0.68167
C-arom-AUA_elec	3.361	35.43	---	0.4	1.355/-0.68167

<sup>†</sup> Lorentz-Berthelot mixing rules were employed to determine the interactions between different force center types. <sup>††</sup>  $\delta$  is the anisotropic distance used in the AUA (Anisotropic United Atoms) potential. <sup>†††</sup>  $\delta_q$  corresponds to the shift between the positive and negative electrostatic charges of the aromatic ring.

### S3.3. Bulk crystal

The bulk zeolite crystals only allow to consider adsorption in the zeolite microporosity. Both the adsorbent and adsorbates are considered as rigid molecules. This assumption has been shown to be valid in previous works considering the adsorption of xylene isomers in zeolitic systems<sup>4</sup>. Since the Si/Al ratio of the X zeolites considered in this work is relatively close to that of their analogous LSX (Low Silica X) forms, the latter forms were considered. In what follows, a brief description of the implementation of the force field is done for the different species of the system.

**NaLSX and BaLSX.** As previously mentioned, for the sake of simplicity, the low silica LSX analogous forms of the NaX and BaX adsorbents are considered. In the same way, the general

assumption of considering rigid the zeolite framework is adopted. The description of the dispersion-repulsion interactions of the framework is considered via a Kiselev type potential.<sup>5</sup> This type of potential assumes that the T atoms (either Si or Al) of the different tetrahedra constituting the zeolite framework are screened by their respective four surrounding oxygen atoms. Concerning the sodium counter-cations, the parameters are taken from the work by Smith and Dang<sup>6</sup>. The barium parameters are calculated following the strategy derived by Maurin et al.<sup>7</sup> The crystallographic positions of the cations were obtained from Pichon et al.<sup>8</sup> To account for the electrostatic interactions, electrostatic point charges were determined from Density Functional Theory (DFT) calculations performed following the approach proposed by Manz *et al*<sup>9</sup>. The different parameters used in the calculations are listed in the Table S3.

**Table S3.** Lennard-Jones parameters and electrostatic point charges for the adsorbents considered in this work.

Force center	$\sigma^\dagger$ [Å]	$\varepsilon/k_b^\dagger$ [K]	$q^{\dagger\dagger}$ [e] NaLSX	$q^{\dagger\dagger}$ [e] BaLSX
O-zeolite	3.00	112.236	-1.2529	-1.2447
Si-zeolite	0.00	0.00	1.9751	2.1439
Al-zeolite	0.00	0.00	2.0728	1.9931
Na	2.584	50.34	0.9770	---
Ba	3.3191	141.789	---	1.6834

<sup>†</sup> Lorentz-Berthelot mixing rules were employed to determine the interactions between different force center types.

<sup>††</sup> Average values.

### S3.4. *NaLSX and BaLSX bearing an external interface*

**Surface selection and preparation.** To the best of our knowledge, no evidence for preferential growth direction in faujasite zeolites is established. Therefore, the surface direction  $\{0\ 1\ 1\}$  was chosen since the cleavage is performed at the level of the  $\alpha$  cages. Figure S7 shows an example of surface cleavage  $\{011\}$ , where the open  $\alpha$  cages can be seen at the surface level. As well-established in the literature, it is possible that such open cavities at the surface level induce an impact on  $px$  selectivity. At high loadings,  $px$  is selectively adsorbed in a site at the center of the dodecagonal window. In the case of the surface  $\{011\}$ , the incomplete dodecagonal window at the surface level can affect  $px$  selectivity. The surface direction  $\{011\}$  cleavage was performed using the Materials Studio software. The parameters used were as follows: cleavage plane  $\{hk1\}$  is equal to  $\{011\}$  with origin (a,b,c) at (0,0,1).

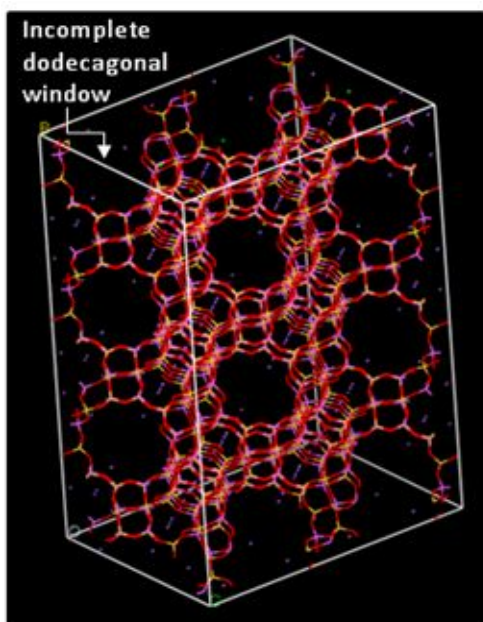


**Figure S7.** Structure of the cleaved surface  $\{011\}$  for a LSX zeolite. The surface  $\{011\}$  cut the  $\alpha$  cages leading to incomplete dodecagonal windows at the surface level.

The chemical reconstruction of the surface was based on IR analyses indicating that silanol groups are located at the outer i.e. external surface. Since the zeolites also exhibit aluminum tetrahedra at the surface level, all bonds missing in the Si or Al tetrahedra were saturated with OH groups after surface cleavage. A similar approach has been reported in the literature.<sup>10</sup> After generating the surfaces by cleaving the bulk zeolite crystal and modifying their surface chemistry, the positions of the atoms in the surface were optimized in order to obtain systems

not bearing any dipole moment contribution. The surfaces have been positioned sufficiently far from each other to ensure that there is no long-range interaction between them.

**Surface force field.** In order to simulate the systems bearing an external interface, the surface atoms need to be parameterized. The adopted strategy consisted in (1) using for the surface atoms the same parameterization as that for bulk atoms and (2) borrowing the electrostatic charges from the CLAYFF potential (as recently done by Purton et al.<sup>11</sup>). Finally, for the dispersion-repulsion parameters, they were obtained from the Universal Force Field (UFF) potential.<sup>12</sup> A list of the different parameters used for the surface oxygen and hydrogen atoms is given in Table S1.

**Table S1.** Lennard-Jones parameters and electrostatic point charges of the zeolite surface.

Force Center	$\sigma^\dagger$ [Å]	$\epsilon/k_b^\dagger$ [K]	q[e]
O-zeolite_surf	3.0000	112.236	-1.0984
H-zeolite_surf	2.5711	22.1418	0.4250

<sup>†</sup> Lorentz-Berthelot mixing rules were employed to determine the interactions between different force center types.

<sup>1</sup> BIOVIA, Dassault Systèmes, Materials Studio, 7.0, San Diego: Dassault Systèmes, 2019

<sup>2</sup> Nieto-Draghi, C.; Bonnaud, P.; Ungerer, P. Anisotropic United Atom Model Including the Electrostatic Interactions of Methylbenzenes. I. Thermodynamic and Structural Properties. *J. Phys. Chem. C* 2007, *111*, 15686–15699

<sup>3</sup> Peralta, D.; Barthelet, K.; Pérez-Pellitero, J.; Chizallet, C.; Chaplais, G.; Simon-Masseron, A.; Pirngruber, G. D. Adsorption and Separation of Xylene Isomers: CPO-27-Ni vs HKUST-1 vs NaY. *J. Phys. Chem. C* 2012, *116*, 21844–21855.

<sup>4</sup> Lachet, V. Simulation moléculaire de l'adsorption sélective des isomères du xylène dans les faujasites, IFPEN, 199

<sup>5</sup> Pascual, P.; Ungerer, P.; Tavitian, B.; Pernot, P.; Boutin, A. Development of a transferable guest–host force field for adsorption of hydrocarbons in zeolites: I. Reinvestigation of alkane adsorption in silicalite by grand canonical Monte Carlo simulation. *Phys. Chem. Chem. Phys.* 2003, *5*, 3684–3693.

<sup>6</sup> Smith, D. E.; Dang, L. X. Computer simulations of NaCl association in polarizable water. *The Journal of Chemical Physics* 1994, *100*, 3757–3766.

<sup>7</sup> Maurin, G.; Llewellyn, P.; Poyet, T.; Kuchta, B. Influence of extra-framework cations on the adsorption properties of X-faujasite systems: Microcalorimetry and molecular simulations. *The journal of physical chemistry. B* 2005, *109*, 125–129.

<sup>8</sup> Pichon, C.; Méthivier, A.; Simonot-Grange, M.-H.; Baerlocher, C. Location of Water and Xylene Molecules Adsorbed on Prehydrated Zeolite BaX. A Low-Temperature Neutron Powder Diffraction Study. *J. Phys. Chem. B* 1999, *103*, 10197–10203

<sup>9</sup> Manz, T. A.; Sholl, D. S.; Chemically Meaningful Atomic Charges That Reproduce the Electrostatic Potential in Periodic and Nonperiodic Materials. *J. Chem. Theory Comput.* 2010, *6*, 2455–2468

<sup>10</sup> Crabtree, J. C.; Molinari, M.; Parker, S. C.; Purton, J. A. Simulation of the Adsorption and Transport of CO<sub>2</sub> on Faujasite Surfaces. *J. Phys. Chem. C* 2013, *117*, 21778–21787

---

<sup>11</sup> Purton, J. A.; Crabtree, J. C.; Parker, S. C. DL\_MONTE: A general purpose program for parallel Monte Carlo simulation. *Molecular Simulation* 2013, *39*, 1240–1252.

<sup>12</sup> Rappe, A. K.; Casewit, C. J.; Colwell, K. S.; Goddard, W. A.; Skiff, W. M. UFF, a full periodic table force field for molecular mechanics and molecular dynamics simulations. *J. Am. Chem. Soc.* 1992, *114*, 10024–10035